

Roles of Modified Chaplygin-Jacobi and Chaplygin-Abel Gases in FRW Universe

Ujjal Debnath *

Department of Mathematics, Indian Institute of Engineering
Science and Technology, Shibpur, Howrah-711 103, India.

December 2, 2021

Abstract

We have considered flat Friedmann-Robertson-Walker (FRW) model of the universe and reviewed the modified Chaplygin gas as the fluid source. Associated with the scalar field model, we have determined the Hubble parameter as a generating function in terms of the scalar field. Instead of hyperbolic function, we have taken Jacobi elliptic function and Abel function in the generating function and obtained modified Chaplygin-Jacobi gas (MCJG) and modified Chaplygin-Abel gas (MCAG) equation of states, respectively. Next, we have assumed that the universe filled in dark matter, radiation, and dark energy. The sources of dark energy candidates are assumed as MCJG and MCAG. We have constrained the model parameters by recent observational data analysis. Using χ^2 minimum test (maximum likelihood estimation), we have determined the best fit values of the model parameters by OHD+CMB+BAO+SNIa joint data analysis. To examine the viability of the MCJG and MCAG models, we have determined the values of the deviations of information criteria like ΔAIC , ΔBIC and ΔDIC . The evolutions of cosmological and cosmographical parameters (like equation of state, deceleration, jerk, snap, lerk, statefinder, Ω_m diagnostic) have been studied for our best fit values of model parameters. To check the classical stability of the models, we have examined the values of square speed of sound v_s^2 in the interval $(0, 1)$ for expansion of the universe.

Keywords: Dark energy, Chaplygin gas, Data analysis, Parameters

arXiv:2112.00296v1 [gr-qc] 1 Dec 2021

*ujjaldebnath@gmail.com

Contents

1	Introduction	2
2	Review of Modified Chaplygin Gas in FRW Model	3
3	Modified Chaplygin-Jacobi Gas	4
4	Modified Chaplygin-Abel Gas	5
5	Observational Data Analysis	6
5.1	OHD	8
5.2	CMB Data	8
5.3	BAO Data	8
5.4	SNIa Data	9
5.5	Information Criteria	10
5.6	Results	10
6	Evolutions of Cosmological and Cosmographical Parameters	13
7	Discussions and Conclusions	16

1 Introduction

From Supernova type Ia [1–3] observation, it has well-established that our universe is undergoing acceleration phase. This is also confirmed by other observations like Baryon Acoustic Oscillation (BAO) [4, 5], Cosmic Microwave Background (CMB) [6], WMAP [7, 8] and Planck [9] observations. There is some unknown matter which possesses sufficient negative pressure (repulsive force), which derives the universe to the acceleration, dubbed as dark energy (DE). According to the most simple and successful candidate of dark energy is the cosmological constant Λ (or vacuum energy) and its density consist of $\sim 70\%$ of total energy density in the universe [10–13]. The concordance Λ cosmology is consistent with the cosmological observations, but it cannot solve the fine-tuning, and the cosmic coincidence problems [11, 12, 14]. So other candidates of dark energy obey time-evolving energy density have been proposed to solve the above cosmological problems [15–18]. The quintessence (or scalar field) [18–25] is another most accepted candidate of DE. There are other scalar field models which are also the candidates of DE models [26–33]. On the other hand, modified theories of gravity may be the alternatives to the DE to derive the acceleration of the universe [34–41].

Another alternative to DE is an exotic type of fluid - the so-called pure Chaplygin gas. The pure Chaplygin gas derives to the present-day acceleration of the universe, which can be treated as a unification of dark matter and DE [42–44]. Then it has been generalized to the generalized Chaplygin gas, which also unifies dark matter and DE [45–47]. Further, it has been modified to the modified Chaplygin gas (MCG), which propagates between radiation and Λ CDM stages [48, 49]. Other extensions of Chaplygin gas are variable Chaplygin gas [50], variable modified Chaplygin gas [51], viscous Chaplygin gas [52] etc., which are also the candidates of DE models that unify dark matter and DE. Due the Supernova, CMBR, WMAP

observations, the parameters of the generalized Chaplygin gas have been constrained [46, 53–55]. Also, the MCG parameters have been constrained by CMBR, WMAP data [56, 57]. On the other hand, the MCG parameters have been constrained in modified gravity theories [58–63].

Villanueva [64] has obtained generalized Chaplygin-Jacobi gas through Hubble parameter associated to the generalized Chaplygin scalar field and using Jacobi’s elliptic function [65]. The relevant inflationary quantities have also been obtained [66]. Motivated by this work, we obtain modified Chaplygin-Jacobi gas and modified Chaplygin-Abel gas equation of states. Then we study the observational data analysis and constrains the model parameters. We check the compatibility of the models with observational data employing AIC, BIC, and DIC model selection tools. Using the best-fitting values of the models’ free parameters, we study the evolutions of cosmological and cosmographical parameters and check the classical stability of the models. The paper is structured as follows. In section 2, we briefly write the basic equations for MCG. In sections 3 and 4, we obtain modified Chaplygin-Jacobi gas and modified Chaplygin-Abel gas equation of states through the Hubble parameter. In section 5, we write the data analysis tools in our constructed models. Then we study the OHD+CMB+BAO+SNIa joint data analysis and the information criteria for our models. Section 4 deals with the evolutions of cosmological and cosmographical parameters using best-fitting values of the model parameters. Finally, in section 7, we discuss the results of the whole work.

2 Review of Modified Chaplygin Gas in FRW Model

The line element for homogeneous and isotropic universe in spatially flat Friedmann-Robertson-Walker (FRW) model is (choosing speed of light $c = 1$)

$$ds^2 = -dt^2 + a^2(t) [dr^2 + r^2(d\theta^2 + \sin^2\theta d\phi^2)] \quad (1)$$

where $a(t)$ is a scale factor depends on time t . The Einstein’s field equations are given by

$$3H^2 = 8\pi G\rho \quad (2)$$

and

$$\dot{H} = -4\pi G(\rho + p) \quad (3)$$

where ρ and p are the energy density and pressure respectively, $H = \dot{a}/a$ denotes the time dependent Hubble parameter and G is the Newtonian gravitational constant. The energy conservation equation is given by

$$\dot{\rho} + 3H(\rho + p) = 0 \quad (4)$$

We consider the fluid source is modified Chaplygin gas (MCG), which obeys the equation of state [48, 49]

$$p = A\rho - \frac{B}{\rho^\alpha} \quad (5)$$

where $A, B(> 0)$ and $\alpha \in (0, 1)$ are constants. We have the solution of ρ as [48, 49]

$$\rho = \left[\frac{B}{1+A} + \frac{C}{a^{3(1+A)(1+\alpha)}} \right]^{\frac{1}{1+\alpha}} \quad (6)$$

where C is an integration constant.

From field-theoretic point of view, we may describe this MCG model by introducing scalar field ϕ and corresponding self-interacting potential $V(\phi)$, which have the effective Lagrangian

$$\mathcal{L}_\phi = \frac{1}{2}\dot{\phi}^2 - V(\phi) \quad (7)$$

The analogous energy density ρ_ϕ and pressure p_ϕ for the scalar field are the following [49]:

$$\rho_\phi = \frac{1}{2}\dot{\phi}^2 + V(\phi) = \rho \quad (8)$$

and

$$p_\phi = \frac{1}{2}\dot{\phi}^2 - V(\phi) = A\rho - \frac{B}{\rho^\alpha} \quad (9)$$

From these equations with the help of field equation (2), we get the solution [49]:

$$\phi = \phi_c + \frac{1}{\sqrt{6\pi G(1+A)(1+\alpha)}} \text{Sinh}^{-1} \left\{ \sqrt{\frac{C(1+A)}{B} \frac{1}{a^{\frac{3}{2}(1+\alpha)(1+A)}}} \right\} \quad (10)$$

where ϕ_c is constant. Using equations (2), (6) and (10), we obtain the generating function for MCG

$$H(\phi) = H_c \text{Sech}^{-\frac{1}{1+\alpha}}(\Phi) \quad (11)$$

where $\Phi = \sqrt{6\pi G(1+A)(1+\alpha)}(\phi - \phi_c)$ and $H_c = \sqrt{\frac{8\pi G}{3}} \left(\frac{B}{1+A} \right)^{\frac{1}{2(1+\alpha)}}$ is the value of the Hubble parameter when $\phi = \phi_c$. Now from equation (3), we get

$$p = -\rho + \frac{1}{(4\pi G)^2} \left(\frac{dH}{d\phi} \right)^2 \quad (12)$$

3 Modified Chaplygin-Jacobi Gas

We know that hyperbolic function is a particular case of elliptic functions and Jacobi elliptic functions are a set of basic elliptic functions. In 2015, Villanueva [64] has replaced the cosine hyperbolic function in the Hubble parameter (obtained by generalized Chaplygin gas) by Jacobi's elliptic function and derived the equation of state, termed as generalized Chaplygin-Jacobi gas. So replacing the hyperbolic function in the generating function (11) by the Jacobi elliptic cosine function $cn(\Phi)$, the generating function can be written as

$$H(\phi) = H_c cn^{-\frac{1}{1+\alpha}}(\Phi) \quad (13)$$

where $cn(\Phi) \equiv cn(\Phi, k)$ and $k \in [0, 1]$ is the elliptic modulus. For $k = 1$, the above equation (13) reduces to the equation (11). Using the relations $cn^2(\Phi) + sn^2(\Phi) = 1$, $cn^2(\Phi) + (1-k)sn^2(\Phi) = dn^2(\Phi)$, $cn'(\Phi) =$

$-sn(\Phi) dn(\Phi)$ (the notations are defined in [64]) and taking the derivative of (13), we obtain

$$\left(\frac{dH}{d\phi}\right)^2 = 6\pi G(1+A)H_c^2 cn^{-\frac{2(2+\alpha)}{1+\alpha}}(\Phi)(1-cn^2(\Phi))((1-k)+k cn^2(\Phi)) \quad (14)$$

Also using equations (8), (9), (12), (13) and (14) we can obtain the potential function

$$V(\phi) = \frac{1}{2} \left(\frac{B}{1+A}\right)^{\frac{1}{2(1+\alpha)}} cn^{-\frac{2}{2+\alpha}}(\Phi)[2+(1-cn^{-2}(\Phi))((1-k)+k cn^2(\Phi))] \quad (15)$$

Using equations (2), (12), (13) and (14), we finally obtain the relation between pressure and density as in the form

$$p = [(2k-1)(1+A)-1]\rho - \frac{kB}{\rho^\alpha} + \frac{(1-k)(1+A)^2}{B} \rho^{2+\alpha} \quad (16)$$

which may be called “*Modified Chaplygin-Jacobi Gas*” (MCJG) equation of state. For $A=0$, the MCJG equation of state can be reduced to the generalized Chaplygin-Jacobi gas equation of state [64]. Putting the expression of p from equation (16) into (4), we obtain

$$\rho^{1+\alpha} = \frac{B}{1+A} \left[\frac{a^{3(1+\alpha)(1+A)} + kD}{a^{3(1+\alpha)(1+A)} - (1-k)D} \right] \quad (17)$$

where D is a positive constant. For large value of scale factor $a(t)$, we have $\rho \simeq \left(\frac{B}{1+A}\right)^{\frac{1}{1+\alpha}}$ and $p \simeq -\left(\frac{B}{1+A}\right)^{\frac{1}{1+\alpha}} = -\rho$ which corresponds to the Λ CDM model with the cosmological constant $= \left(\frac{B}{1+A}\right)^{\frac{1}{1+\alpha}}$. But on the other hand, in the phase of the universe where $x = a^{3(1+\alpha)(1+A)} - (1-k)D \simeq 0$, we have $\rho \simeq \left(\frac{B}{1+A} \frac{D}{x}\right)^{\frac{1}{1+\alpha}}$. This corresponds to a phase of the universe which follows polytropic equation of state $p = \frac{(1-k)(1+A)}{B} \rho^{\alpha+2}$. The above expression of ρ can be written in the following form

$$\rho^{1+\alpha} = \frac{B}{1+A} \left[\frac{A_s + (1-A_s)(1+z)^{3(1+\alpha)(1+A)}}{kA_s - (1-k)(1-A_s)(1+z)^{3(1+\alpha)(1+A)}} \right] \quad (18)$$

where $A_s = \frac{1}{1+kD}$ satisfying $1-k < A_s < 1$. So the present value of the energy density is $\rho_{CJ0}^{1+\alpha} = \frac{B}{(1+A)[kA_s - (1-k)(1-A_s)]}$. The equation of state (EoS) parameter is obtained in the form

$$W = \frac{p}{\rho} = [(2k-1)(1+A)-1] - k(1+A) \left[\frac{kA_s - (1-k)(1-A_s)(1+z)^{3(1+\alpha)(1+A)}}{A_s + (1-A_s)(1+z)^{3(1+\alpha)(1+A)}} \right] \\ + (1-k)(1+A) \left[\frac{A_s + (1-A_s)(1+z)^{3(1+\alpha)(1+A)}}{kA_s - (1-k)(1-A_s)(1+z)^{3(1+\alpha)(1+A)}} \right] \quad (19)$$

4 Modified Chaplygin-Abel Gas

Abel elliptic functions are a special kind of elliptic function. If we replace the hyperbolic function in the generating function (11) by the Abel elliptic function $F(\Phi)$, the generating function (11) in terms of Abel elliptic function can be written as

$$H(\phi) = H_c F^{-\frac{1}{1+\alpha}}(\Phi) \quad (20)$$

Here $F(\Phi) = \sqrt{1 + e^2 \varphi^2(\Phi)}$ where $\varphi(\Phi) \equiv \varphi(\Phi, c, e)$ is also Abel elliptic function (here $c, e \in \mathbb{R}$). Using the relation $\varphi'(\Phi) = \sqrt{(1 - c^2 \varphi^2(\Phi))(1 + e^2 \varphi^2(\Phi))}$ and taking the derivative of (20), we obtain

$$\left(\frac{dH}{d\phi}\right)^2 = 6\pi G(1+A)H_c^2 F^{-\frac{2(2+\alpha)}{1+\alpha}}(\Phi)(F^2(\Phi) - 1)((c^2 + e^2) - c^2 F^2(\Phi)) \quad (21)$$

Also using equations (8), (9), (12), (20) and (21) we can obtain the potential function

$$V(\phi) = \frac{1}{2} \left(\frac{B}{1+A}\right)^{\frac{1}{2(1+\alpha)}} F^{-\frac{2}{2+\alpha}}(\Phi)[2 + (F^{-2}(\Phi) - 1)((c^2 + e^2) - c^2 F^2(\Phi))] \quad (22)$$

Using equations (2), (12), (20) and (21), we finally obtain the relation between pressure and density as in the form

$$p = [(e^2 + 2c^2)(1+A) - 1]\rho - \frac{c^2 B}{\rho^\alpha} - \frac{(e^2 + c^2)(1+A)^2}{B} \rho^{2+\alpha} \quad (23)$$

which may be called “*Modified Chaplygin-Abel Gas*” (MCAG) equation of state. For $A = 0$, the MCAG equation of state may be called the generalized Chaplygin-Abel gas equation of state. Putting the expression of p from equation (23) into (4), we obtain

$$\rho^{1+\alpha} = \frac{B}{1+A} \left[\frac{a^{3e^2(1+\alpha)(1+A)} + c^2 K}{a^{3e^2(1+\alpha)(1+A)} + (e^2 + c^2)K} \right] \quad (24)$$

where K is a positive constant. For large value of scale factor $a(t)$, we obtain $p \simeq -\rho$ which corresponds to the Λ CDM model with the cosmological constant $= \left(\frac{B}{1+A}\right)^{\frac{1}{1+\alpha}}$. For small value of scale factor $a(t)$, we also obtain $p \simeq -\rho$, which corresponds to the inflationary stage of the universe. So the MCAG propagates between inflation and Λ CDM stages. The above expression of ρ can be written in the form

$$\rho^{1+\alpha} = \frac{c^2 B}{1+A} \left[\frac{B_s + (1 - B_s)(1+z)^{3e^2(1+\alpha)(1+A)}}{c^2 B_s + (e^2 + c^2)(1 - B_s)(1+z)^{3e^2(1+\alpha)(1+A)}} \right] \quad (25)$$

where $B_s = \frac{1}{1+c^2 K}$ satisfying $0 < B_s < 1$. So the present value of the energy density is $\rho_{CA0}^{1+\alpha} = \frac{c^2 B}{(1+A)[c^2 B_s + (e^2 + c^2)(1 - B_s)]}$. The equation of state (EoS) parameter is obtained in the form

$$W = \frac{p}{\rho} = [(e^2 + 2c^2)(1+A) - 1] - (1+A) \left[\frac{c^2 B_s + (e^2 + c^2)(1 - B_s)(1+z)^{3e^2(1+\alpha)(1+A)}}{B_s + (1 - B_s)(1+z)^{3e^2(1+\alpha)(1+A)}} \right] - c^2(e^2 + c^2)(1+A) \left[\frac{B_s + (1 - B_s)(1+z)^{3e^2(1+\alpha)(1+A)}}{c^2 B_s + (e^2 + c^2)(1 - B_s)(1+z)^{3e^2(1+\alpha)(1+A)}} \right] \quad (26)$$

5 Observational Data Analysis

Now, we assume that the universe is composed of radiation, dark matter (DM), and dark energy (DE). So in the Einstein field equations (2), (3) and in the conservation equation (4), we can consider $\rho = \rho_r + \rho_m + \rho_d$ and $p = p_r + p_m + p_d$. Here suffices r, m, d denote the radiation, dark matter, and dark energy, respectively. If we assume that there is no interaction between radiation, DM, and DE, then their conservation equations

will be

$$\dot{\rho}_r + 3H(\rho_r + p_r) = 0, \quad (27)$$

$$\dot{\rho}_m + 3H(\rho_m + p_m) = 0 \quad (28)$$

and

$$\dot{\rho}_d + 3H(\rho_d + p_d) = 0 \quad (29)$$

For radiation, the EoS is $p_r = \frac{1}{3}\rho_r$, so from equation (27) we get the solution $\rho_r = \rho_{r0}(1+z)^4$. Also since the DM has negligible pressure (i.e., $p_m \approx 0$), so from equation (28) we obtain the solution $\rho_m = \rho_{m0}(1+z)^3$. Here ρ_{r0} and ρ_{m0} represent the present values of radiation density and DM density, respectively. Next we assume that the DE of the universe is in the form of MCJG or MCAG.

• **MCJG** : If the DE of the universe obeys the MCJG equation of state (16), then using the equation (18), the equation (2) reduces to the following equation for $E(z)$ as

$$E^2(z) = \Omega_{r0}(1+z)^4 + \Omega_{m0}(1+z)^3 + \Omega_{CJ0}[kA_s - (1-k)(1-A_s)]^{\frac{1}{1+\alpha}} \times \left[\frac{A_s + (1-A_s)(1+z)^{3(1+\alpha)(1+A)}}{kA_s - (1-k)(1-A_s)(1+z)^{3(1+\alpha)(1+A)}} \right]^{\frac{1}{1+\alpha}} \quad (30)$$

where we have defined the normalized Hubble parameter $E(z) = \frac{H(z)}{H_0}$ and the dimensionless density parameters $\Omega_{r0} = \frac{8\pi G\rho_{r0}}{3H_0^2}$, $\Omega_{m0} = \frac{8\pi G\rho_{m0}}{3H_0^2}$ and $\Omega_{CJ0} = \frac{8\pi G\rho_{CJ0}}{3H_0^2}$. Putting $z = 0$ in the above equation, we obtain $\Omega_{r0} + \Omega_{m0} + \Omega_{CJ0} = 1$.

• **MCAG** : If the DE of the universe obeys the MCAG equation of state (23), then using the equation (25), the equation (2) reduces to the following equation for $E(z)$ as

$$E^2(z) = \Omega_{r0}(1+z)^4 + \Omega_{m0}(1+z)^3 + \Omega_{CA0}[c^2B_s + (e^2 + c^2)(1-B_s)]^{\frac{1}{1+\alpha}} \times \left[\frac{B_s + (1-B_s)(1+z)^{3e^2(1+\alpha)(1+A)}}{c^2B_s + (e^2 + c^2)(1-B_s)(1+z)^{3e^2(1+\alpha)(1+A)}} \right]^{\frac{1}{1+\alpha}} \quad (31)$$

where the dimensionless density parameter $\Omega_{CA0} = \frac{8\pi G\rho_{CA0}}{3H_0^2}$. Putting $z = 0$ in the above equation, we obtain $\Omega_{r0} + \Omega_{m0} + \Omega_{CA0} = 1$.

In this section, we'll study the observational data analysis tools for fitting the theoretical MCJG and MCAG models in flat FRW universe. To determine the best fit values of the unknown parameters of the models, we use the observed Hubble data (OHD), cosmic microwave background (CMB) data, baryonic acoustic oscillations (BAO) data and type Ia supernova (SNIa) data survey. For this purpose, we use minimum values of χ^2 with maximum likelihood analysis using different confidence levels (like 1σ , 2σ and 3σ) due to OHD+CMB+BAO+SNIa observational data.

5.1 OHD

Due to latest observed Hubble data (OHD) sets compilation [67–69] with 57 data points in the region $0.07 \lesssim z \lesssim 2.42$ [70], the χ^2 value (as a sum of standard normal distribution) can be written as

$$\chi_{OHD}^2 = \sum \frac{(H(z) - H_{obs}(z))^2}{\sigma_{obs}^2(z)} \quad (32)$$

where $H(z)$ and $H_{obs}(z)$ respectively represent the theoretical and observed values of the Hubble parameter. Also $\sigma_{obs}(z)$ refers to the standard error in the observed value of H . Due to Planck 2015 results [9], we take a prior for the present value of the Hubble constant $H_0 = 67.8 \text{ km/s/MPc}$.

5.2 CMB Data

To constraints the dark energy, we use the Cosmic Microwave Background (CMB) anisotropy spectrum at the last scattering surface at the redshift $z \simeq 1100$. So we use the Planck distance priors from the Planck 2015 data sets [9]. The proper angular diameter distance $D_A(z)$, CMB shift parameter \mathcal{R} , comoving sound horizon size $r_s(z)$ and acoustic scale parameter ℓ_A are respectively given by [71, 72]

$$D_A(z) = \frac{1}{H_0(1+z)} \int_0^z \frac{dz'}{E(z')}, \quad (33)$$

$$\mathcal{R} = H_0 \sqrt{\Omega_{m0}} (1+z_*) D_A(z_*), \quad (34)$$

$$r_s(z) = \frac{1}{H_0} \int_0^x \frac{dx'}{x' E(x') \sqrt{3(1 + \bar{R}_b x')}} \quad (35)$$

and

$$\ell_A = (1+z_*) \frac{\pi D_A(z_*)}{r_s(z_*)} \quad (36)$$

where $\bar{R}_b x = 0.75 \rho_b / \rho_\gamma$. The ρ_b and ρ_γ are respectively the baryon energy density and photon energy density at the present epoch. Also, the baryon density is $\omega_b = \Omega_{b0} h^2$ [71, 73]. The z_* is the redshift in the CMB power spectrum at the last scattering surface, given by the fitting formula [71, 73]

$$z_* = 1048 \left[1 + 0.00124 (\Omega_{b0} h^2)^{-0.738} \right] \left[1 + \frac{0.0783 (\Omega_{b0} h^2)^{-0.238}}{1 + 39.5 (\Omega_{b0} h^2)^{-0.76}} (\Omega_{m0} h^2)^{\frac{0.560}{1+21.1(\Omega_{b0} h^2)^{1.81}}} \right] \quad (37)$$

The χ^2 function for CMB measurement, is defined by [9, 71]

$$\chi_{CMB}^2 = \Delta S_i [Cov_{CMB}^{-1}(S_i, S_j)] \Delta S_j, \quad \Delta S_i = S_i^{theory} - S_i^{obs} \quad (38)$$

where $S_1 = \ell_A$, $S_2 = \mathcal{R}$, $S_3 = \omega_b$ and Cov^{-1} is the inverse covariance matrix. The CMB data does not provide the full Planck information, but it is an optimum way of studying several dark energy models.

5.3 BAO Data

Eisenstein et al. [4, 5] proposed the Baryon Acoustic Oscillation (BAO) observational data analysis. BAO refers to the imprint left by relativistic sound waves in the early universe, providing an observable to the late-time large-scale structure. BAO measures the structures in the universe from very large scales at different

times (i.e., redshifts). For BAO measurement, the effective distance measure $D_V(z)$ is defined by [71, 72]

$$D_V(z) = \left[(1+z)^2 D_A^2(z) \frac{z}{H(z)} \right]^{1/3} \quad (39)$$

The comoving sound horizon size $r_s(z_d)$ is given in equation (35), where z_d is the redshift at the drag epoch given by [4, 71]

$$z_d = \frac{1291 (\Omega_{m0} h^2)^{0.251}}{1 + 0.659 (\Omega_{m0} h^2)^{0.828}} \left[1 + 0.313 (\Omega_{m0} h^2)^{-0.419} (\Omega_{b0} h^2)^{0.238} (\Omega_{m0} h^2)^{0.223} \left[1 + 0.607 (\Omega_{m0} h^2)^{0.674} \right] \right] \quad (40)$$

For our data analysis, we use four data points: (i) for 6dF Galaxy Survey [74], $r_s(z_d)/D_V(0.106) = 0.336 \pm 0.015$; (ii) for SDSS-DR7 [75], $D_V(0.15) = (664 \pm 25 \text{ Mpc})(r_d/r_{d, fid})$; (iii) for BOSS-DR11 [76], $D_V(0.32) = (1264 \pm 25 \text{ Mpc})(r_d/r_{d, fid})$ and (iv) for BOSS-DR11 [76], $D_V(0.57) = (2056 \pm 20 \text{ Mpc})(r_d/r_{d, fid})$. The χ^2 function for BAO measurement, is defined by [71]

$$\chi_{BAO}^2 = \Delta S_i [Cov_{BAO}^{-1}(S_i, S_j)] \Delta S_j, \quad \Delta S_i = S_i^{theory} - S_i^{obs} \quad (41)$$

5.4 SNIa Data

The most important and key class of cosmological probes is the standard candles, in which most known standard candles are Supernovae Type Ia (SNIa). For SNIa observation, the luminosity distance $d_L(z)$ and distance modulus $\mu(z)$ are given by [2, 3, 77, 78]

$$d_L(z) = (1+z) \int_0^z \frac{dz'}{E(z')} \quad (42)$$

and

$$\mu(z) = 5 \log_{10} \left[\frac{d_L(z)/H_0}{1 \text{ Mpc}} \right] + 25 \quad (43)$$

From SDSS-II sample, SNLS sample and few high redshift samples from HST (Hubble Space Telescope) with 740 data points [79] with redshift z lies in the region $0.01 \leq z \leq 1.30$, the χ^2 function for JLA (joint light-curve analysis) compilation can be written as [80–83]

$$\chi_{SN}^2 = A_{SN} - \frac{B_{SN}^2}{C_{SN}} \quad (44)$$

where

$$A_{SN} = \sum_{i=1}^{740} \frac{[\mu_{th}(z_i) - \mu_{obs}(z_i)]^2}{\sigma^2(z_i)}, \quad B_{SN} = \sum_{i=1}^{740} \frac{[\mu_{th}(z_i) - \mu_{obs}(z_i)]}{\sigma^2(z_i)}, \quad C_{SN} = \sum_{i=1}^{740} \frac{1}{\sigma^2(z_i)} \quad (45)$$

The total χ^2 function for OHD+CMB+BAO+SNIa joint data analysis can be written as

$$\chi^2 = \chi_{OHD}^2 + \chi_{CMB}^2 + \chi_{BAO}^2 + \chi_{SN}^2 \quad (46)$$

Using the χ^2 minimum test, we can determine the best fit values of the parameters of MCJG and MCAG in the FRW universe. Since the MCJG and MCAG models have a different number of parameters, so it is very difficult to a fair comparison between these DE models by directly comparing their χ^2 values. Obviously, a

DE model involves more parameters that have a lower value of χ^2 . So to discuss the fair model comparison, we need to study the information criteria in the following subsection.

5.5 Information Criteria

Since the MCJG and MCAG have several parameters, so to discuss the analysis, we need to know the information criteria (IC). The Akaike Information Criteria (AIC) [84], Bayesian Information Criteria (BIC) [85] and Deviance Information Criterion (DIC) [86, 87] are more popular among ICs. Since AIC was derived by an approximate minimization of Kullback-Leibler information, so AIC is an asymptotically unbiased estimator of Kullback-Leibler information. In the standard assumption of Gaussian errors, the corresponding Gaussian estimator for the AIC can be written as [87–90] $AIC = -2\ln(\mathcal{L}_{max}) + 2\kappa + \frac{2\kappa(\kappa+1)}{N-\kappa-1}$ where \mathcal{L}_{max} is the maximum likelihood function, κ is the number of model parameters, and N is the number of data points used in the data fit. Since $N \gg 1$, so the above expression reduces to the original AIC version: $AIC = -2\ln(\mathcal{L}_{max}) + 2\kappa$. Also, the Bayesian estimator for BIC can be defined as [87–89] $BIC = -2\ln(\mathcal{L}_{max}) + \kappa \ln N$. We see that the BIC is similar to AIC with a different second term. For the given set of models, the deviations of the IC values are $\Delta AIC = AIC_{model} - AIC_{min} = \Delta\chi_{min}^2 + 2\Delta\kappa$ and $\Delta BIC = BIC_{model} - BIC_{min} = \Delta\chi_{min}^2 + \Delta\kappa \ln N$. For data analysis, the extensively favorable range of ΔAIC is (0, 2). The less support range of ΔAIC is (4, 7), but when $\Delta AIC > 10$, the model provides no support. For a model, ΔBIC of 2 provides positive evidence against the model with higher BIC while ΔBIC of 6 supports strong evidence. On the other hand, the concepts of both Bayesian statistics and information theory, the DIC can be defined as [86, 87] $DIC = 2\overline{D(\theta)} - D(\bar{\theta})$ where $D(\theta) = -2\ln(\mathcal{L}(\theta)) + C$. Here C is a standard constant depending only on the data which will vanish from any derived quantity, D is the deviance of the likelihood function, and bar denotes the mean value of the posterior distribution. For deviation of the DIC value $\Delta DIC = DIC_{model} - DIC_{min}$, the lower value (< 2) provides strong support of the model, instead of the higher value of ΔDIC (less support). It should be noted that the AIC and BIC count all the involved parameters of the model, but DIC counts only the number of parameters of the model that contribute to the fit in an actual way.

5.6 Results

In the MCJG and MCAG models, the best fit values of the parameters can be obtained by χ^2 minimum test using the maximum likelihood estimation. The parameter of the radiation density is given by the formula $\Omega_{r0} = \Omega_{m0}/(1 + z_{eq})$ where $z_{eq} = 2.5 \times 10^4 \Omega_{m0} h^2 (T_{cmb}/2.7K)^{-4}$. Now we choose $\Omega_{rad0} = 8.14 \times 10^{-5}$. Using OHD+CMB+BAO+SN Ia joint data analysis, the best fit parameters for MCJG and MCAG modes are obtained by (i) $\Omega_{m0} = 0.328$, $h = 0.657$, $\alpha = 0.066$, $A = 0.297$, $A_s = 0.586$, $k = 0.521$, $\chi_{min}^2 = 657.381$ and (ii) $\Omega_{m0} = 0.317$, $h = 0.631$, $\alpha = 0.063$, $A = 0.276$, $B_s = 0.527$, $e = 0.172$, $c = 0.392$, $\chi_{min}^2 = 632.197$ respectively. The best fit results with errors of the model parameters are also given in Tables 1 and 2. In the figures 1 - 4, we have drawn the contour plots of h vs Ω_{m0} , α vs A_s , A vs A_s and k vs A_s for MCJG by OHD+CMB+BAO+SN Ia joint data analysis for 1σ , 2σ and 3σ confidence levels. Also in the figures 5 - 9, we have plotted the contours of h vs Ω_{m0} , α vs B_s , A vs B_s , e vs B_s and c vs B_s for MCAG model. Since Λ CDM model is the reference model, so the values of ΔAIC , ΔBIC and ΔDIC

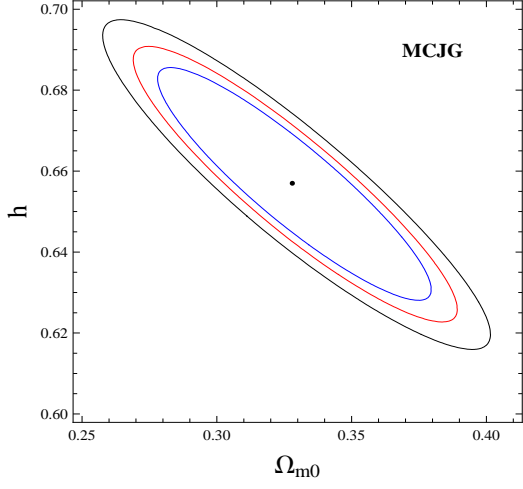


Fig.1

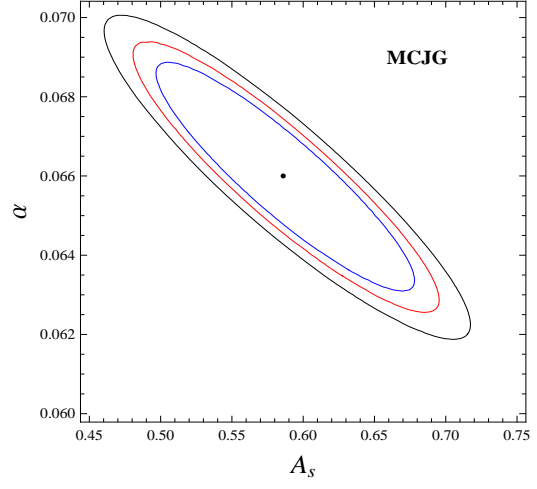


Fig.2

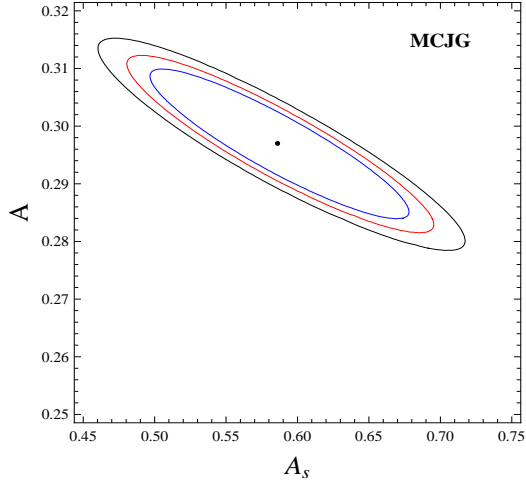


Fig.3

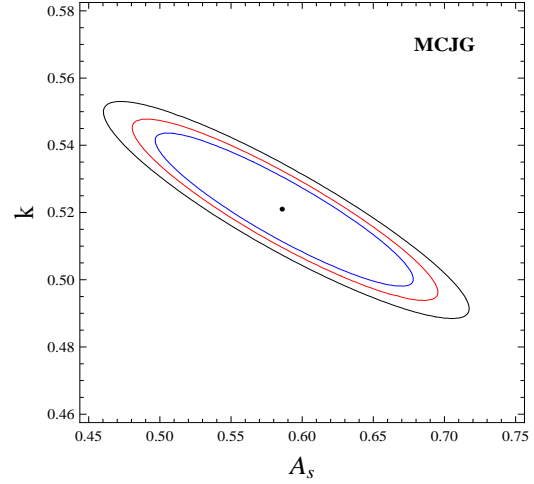


Fig.4

Figs.1 - 4: Contour plots of h vs Ω_{m0} , α vs A_s , A vs A_s and k vs A_s for MCJG by OHD+CMB+BAO+SNIa joint data analysis for different confidence levels 1σ (blue), 2σ (red) and 3σ (black).

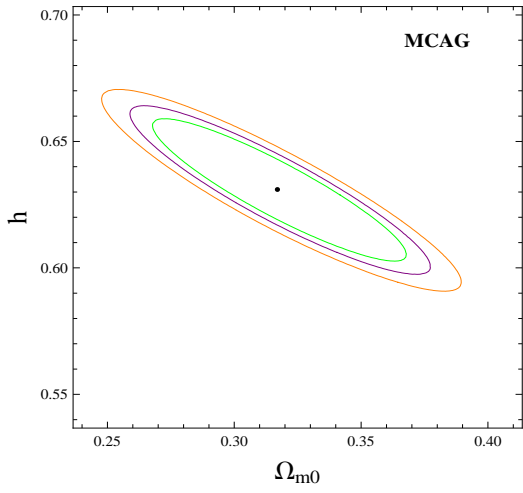


Fig.5

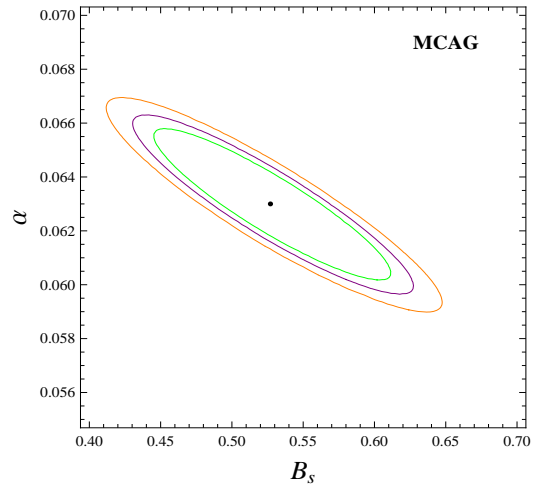


Fig.6

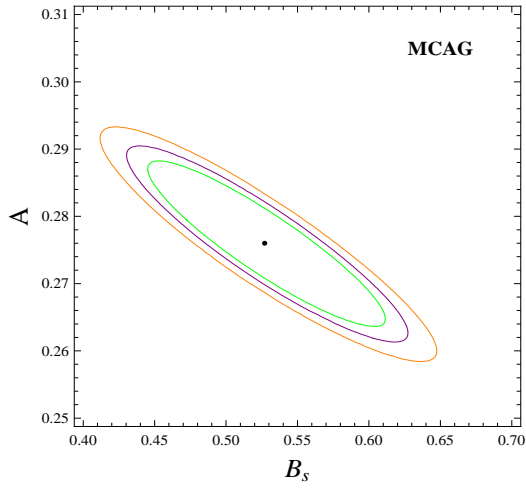


Fig.7

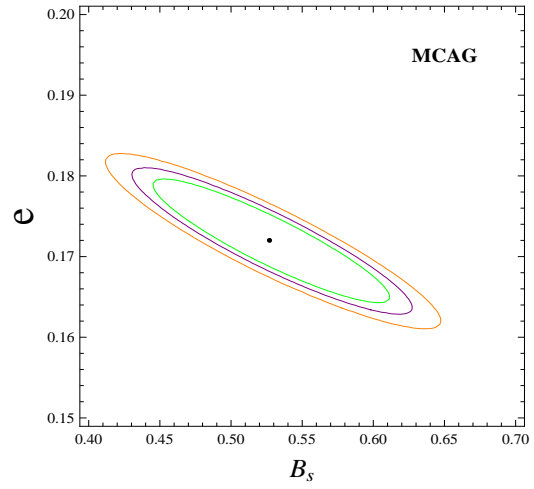


Fig.8

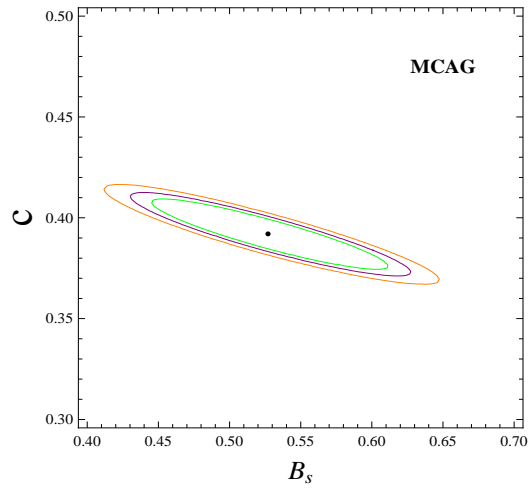


Fig.9

Figs.5 - 9: Contour plots of h vs Ω_{m0} , α vs B_s , A vs B_s , e vs B_s and c vs B_s for MCAG by OHD+CMB+BAO+SN Ia joint data analysis for different confidence levels 1σ (green), 2σ (purple) and 3σ (orange).

for MCJG and MCAG models can be measured relative to the Λ CDM model. For Λ CDM model, we know that $\Delta\text{AIC}=\Delta\text{BIC}=\Delta\text{DIC}=0$ [71]. But for MCJG and MCAG models, we found (i) $\Delta\text{AIC}=1.293$, $\Delta\text{BIC}=5.824$, $\Delta\text{DIC}=1.096$ and (ii) $\Delta\text{AIC}=1.131$, $\Delta\text{BIC}=5.795$, $\Delta\text{DIC}=1.072$ which lie on the favorable ranges. So we can conclude that the MCJG and MCAG models are observationally viable models.

Model	Ω_{m0}	h	α	A	A_s	k	χ^2_{min}
MCJG	$0.328^{+0.049}_{-0.047}$	$0.657^{+0.028}_{-0.027}$	$0.066^{+0.0025}_{-0.0026}$	$0.297^{+0.011}_{-0.012}$	$0.586^{+0.09}_{-0.08}$	$0.521^{+0.019}_{-0.021}$	657.381

Table 1: Best fit results of the MCJG model parameters by OHD+CMB+BAO+SN Ia joint data analysis.

Model	Ω_{m0}	h	α	A	B_s	e	c	χ^2_{min}
MCAG	$0.317^{+0.043}_{-0.049}$	$0.631^{+0.024}_{-0.023}$	$0.063^{+0.0025}_{-0.0023}$	$0.276^{+0.012}_{-0.013}$	$0.527^{+0.075}_{-0.077}$	$0.172^{+0.007}_{-0.008}$	$0.392^{+0.018}_{-0.017}$	632.197

Table 2: Best fit results of the MCAG model parameters by OHD+CMB+BAO+SN Ia joint data analysis.

6 Evolutions of Cosmological and Cosmographical Parameters

In this section, we'll study the nature of the cosmological and cosmographical parameters due to taking the best fit values of the parameters of MCJG and MCAG models. The propagations of MCJG and MCAG for the evolution of the universe can be determined by the equation of state parameter W . From figure 10, we see that W decreases from positive level $W > 0$ to $W \sim 0$, i.e., radiation to dust models can be generated for both MCJG and MCAG. Then W decreases and keeps negative sign ($-1 < W < 0$), i.e., quintessence models can be generated. Here $W < -1/3$ shows the dark energy phase of the universe. Finally, W reaches to -1 as $z \sim -1$, i.e., the universe goes to the Λ CDM stages due to the contributions of MCJG and MCAG. At the early stage of the universe, the value of W for MCAG is higher than MCJG. Obviously, at $z = 0$, the value of W lies within -1 and -0.8 . So at present, our universe is accelerating, which may be caused by both MCJG and MCAG. Since $W \not< -1$, so phantom crossing cannot occur in our considered MCJG and MCAG models.

In order to deceleration or acceleration phase of the universe, we need to study the deceleration parameter, which is given as $q = -\frac{\ddot{a}}{aH^2}$. For the deceleration phase of the universe, $q > 0$ and for the acceleration phase of the universe, $q < 0$. The deceleration parameter has been drawn in figure 11 for both MCJG and MCAG. As time passes, we see that q decreases from positive level to negative level, i.e., deceleration to acceleration transition occurs to the universe. There are another parameters named as cosmographical parameters for understanding the past and future evolution of the universe. The cosmography is the study of scale factor by expanding it by Taylor series with respect to the cosmic time. The cosmographical parameter

like jerk (J), snap (S), and lerk (L) parameters are [91–94]

$$J = \frac{\ddot{a}}{aH^3} = (1+z)\frac{dq}{dz} + q(1+2q), \quad (47)$$

$$S = \frac{a^{(4)}}{aH^4} = -(1+z)\frac{dJ}{dz} - J(2+3q), \quad (48)$$

$$L = \frac{a^{(5)}}{aH^5} = -(1+z)\frac{dS}{dz} - S(3+4q) \quad (49)$$

So the cosmographical parameters are higher-order derivatives of deceleration parameter q . We have drawn the jerk (J), snap (S) and lerk (L) parameters in figures 12, 13 and 14 respectively for both MCJG and MCAG models. The parameters J and L both decrease sharply from some positive values to near-zero upto $z \sim 1$ and then increase sharply upto some positive values. The sharpness of decrease and increase curves for MCAG is higher than MCJG. On the other hand, the parameter S increases from negative level to positive level, and the transition occurs near $z = 1$. The sharpness of decrease and increase curves for MCAG is higher than MCJG.

Another important parameters are statefinder parameters which are distinguishing different dark energy models. The statefinder parameters $\{r, s\}$ are defined as [95, 96]

$$r = \frac{\ddot{a}}{aH^3}, \quad s = \frac{r-1}{3(q-0.5)} \quad (50)$$

For Λ CDM model, $\{r, s\} = \{0, 1\}$ and for SCDM model, $\{r, s\} = \{1, 1\}$. The $\{r, s\}$ trajectory is drawn in figure 15. We see that when r increases, s always decreases. Two branches of the trajectory found in the diagram. Two branches intersect at $r = 1, s = 0$. For $s > 0$, the value of r is < 1 . In this region, the lower value of r is ~ 0.4 and the corresponding upper value of s is ~ 0.2 . But for $s < 0$, the value of r is > 1 for both MCJG and MCAG models.

The Om diagnostic of dark energy is the first derivative of the scale factor through the Hubble parameter, was introduced to differentiate Λ CDM from other DE models, which is defined as [97]

$$Om(x) = \frac{E^2(x) - 1}{x^3 - 1} \quad (51)$$

where $x = z + 1$. For Λ CDM model, $Om = \Omega_{0m} = \text{constant}$. The Om diagnostic against redshift z is plotted in figure 16. We see that in the region $z > 0$, the Om parameter decreases from some positive values to nearly zero around $z \sim 0$. But for $z < 0$, the Om parameter obeys the negative signature for both MCJG and MCAG.

Finally, we can examine whether the MCJG and MCAG are stable or not for the best fit values of the parameters. So to study the stability of MCJG and MCAG against small perturbation, we can write the squared speed of sound in the form $v_s^2 = \frac{dp}{d\rho}$. If $0 < v_s^2 < 1$, we can say that the model is classically stable while $v_s^2 < 0$ or $v_s^2 > 1$ represents classically unstable. The square speed of sound v_s^2 is drawn in figure 17. We observe that v_s^2 decreases smoothly but lies within 0.2 and 0.82. So we can conclude that MCJG and MCAG are classically stable due to taking the best fit values of the model's parameters.

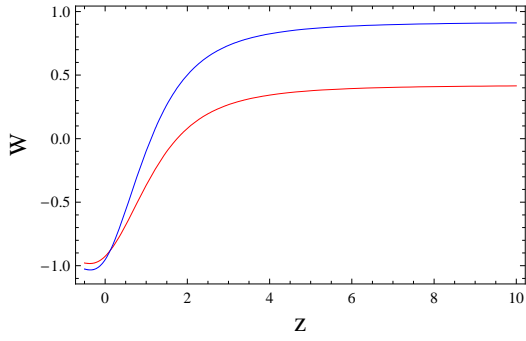


Fig.10

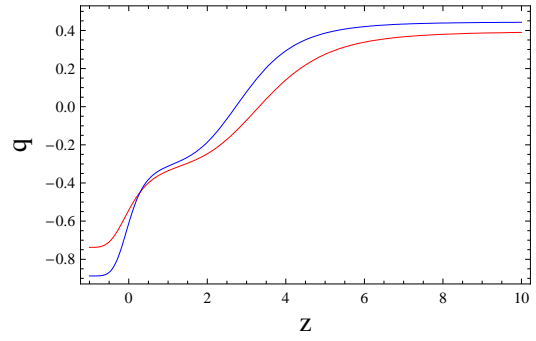


Fig.11

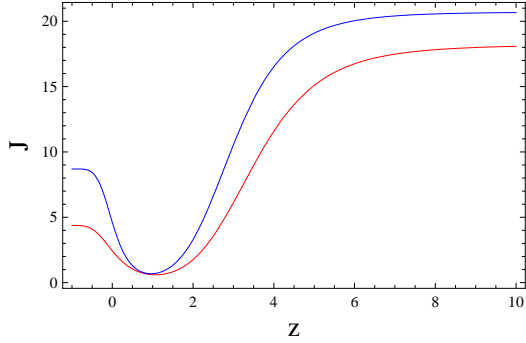


Fig.12

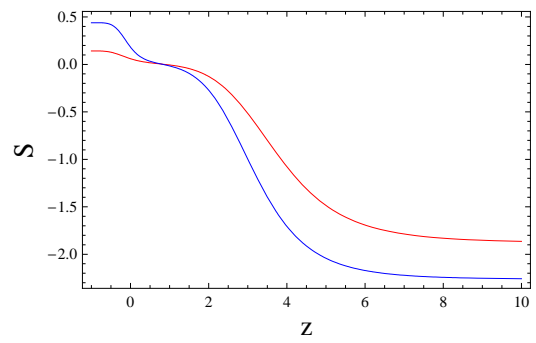


Fig.13

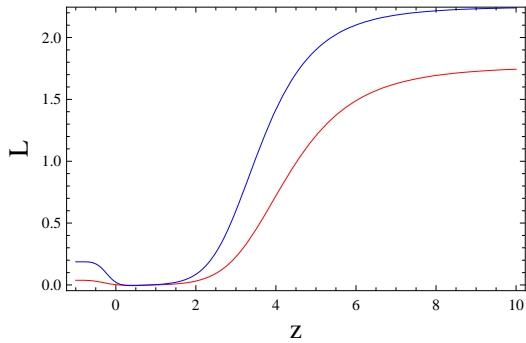


Fig.14

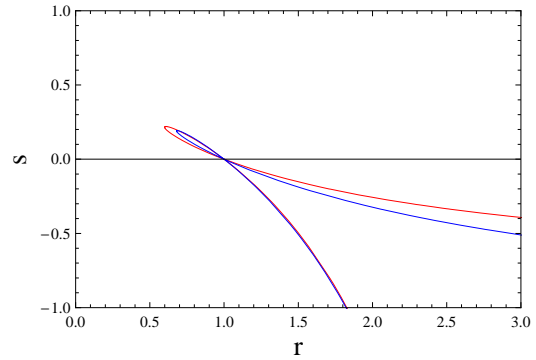


Fig.15

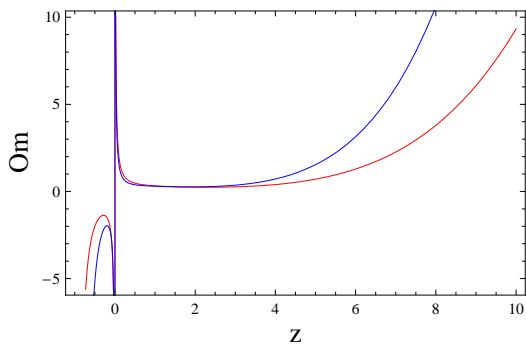


Fig.16

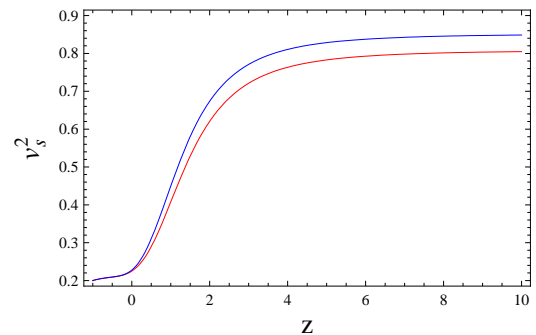


Fig.17

Figs.10 - 17: Plots of W , q , J , S , L vs z , s vs r , Om and v_s^2 vs z for MCJG (red line) and MCAG (blue line).

7 Discussions and Conclusions

We have considered the flat FRW model of the universe and reviewed the modified Chaplygin gas as the fluid source. Associated with the scalar field model, we have determined the Hubble parameter as a generating function in terms of the scalar field. Instead of hyperbolic function, we have taken Jacobi elliptic function and Abel function in the generating function and obtained modified Chaplygin-Jacobi gas (MCJG) and modified Chaplygin-Abel gas (MCAG) equation of states, respectively. Next, we have assumed that the universe filled in dark matter, radiation, and dark energy. The sources of dark energy candidates are assumed as MCJG and MCAG. We have constrained the model parameters by recent observational data analysis. Using χ^2 minimum test (maximum likelihood estimation), we have determined the best fit values of the model parameters by OHD+CMB+BAO+SNIa joint data analysis. In the figures 1 - 4, we have drawn the contour plots of h vs Ω_{m0} , α vs A_s , A vs A_s and k vs A_s for MCJG model in 1σ , 2σ and 3σ confidence levels. Also, in figures 5 - 9, we have plotted the contours of h vs Ω_{m0} , α vs B_s , A vs B_s , e vs B_s and c vs B_s for MCAG model. To examine the viability of the MCJG and MCAG models, we have determined the values of the deviations of information criteria like ΔAIC , ΔBIC and ΔDIC . Since ΛCDM model is the reference model, so the values of ΔAIC , ΔBIC , and ΔDIC for MCJG and MCAG models can be measured relative to the ΛCDM model. Our computational values of ΔAIC , ΔBIC , and ΔDIC lie on the favorable ranges. So our constructed MCJG and MCAG are observationally favorable models.

The evolutions of cosmological and cosmographical parameters (like equation of state, deceleration, jerk, snap, lerk, statefinder, Om diagnostic) have been studied using best-fit values of MCJG and MCAG parameters. From figure 10, we have seen that the EoS parameter W decreases from positive level $W > 0$ to $W = -1$, i.e., radiation to ΛCDM models can be generated for both MCJG and MCAG. But at the early stage of the universe, the value of W for MCAG is higher than MCJG. At present, our universe is accelerating, which may be caused by MCJG and MCAG. Since $W \not< -1$, so phantom divide cannot occur in our considered MCJG and MCAG models. Also, for both MCJG and MCAG models, from figure 11, we have seen that the deceleration parameter q decreases from positive level to negative level, i.e., deceleration to acceleration phase transition occurs to the universe. We have drawn the jerk (J), snap (S), and lerk (L) parameters in figures 12, 13, and 14, respectively, for both MCJG and MCAG models. The parameters J and L decrease sharply from some positive values to near-zero upto $z \sim 1$ and then increase sharply upto some positive values. The sharpness of decrease and increase curves for MCAG is higher than MCJG. On the other hand, S increases from negative level to positive level, and the transition occurs near $z = 1$. The sharpness of decrease and increase of the trajectories for MCAG is higher than MCJG. From figure 15, we have seen that when r increases, s always decreases. Two branches of the trajectory found in the (r, s) diagram. Two branches intersect at $r = 1$, $s = 0$. For $s > 0$, the value of r is < 1 . In this region, the lower value of r is ~ 0.4 and the corresponding upper value of s is ~ 0.2 . But for $s < 0$, the value of r is > 1 for both MCJG and MCAG models. On the other hand, from figure 16, we have seen that in the region $z > 0$, the Om parameter decreases from some positive values to nearly zero around $z \sim 0$, while for $z < 0$, Om parameter obeys negative signature for both MCJG and MCAG. To check the classical stability of the models, we have examined the values of square speed of sound v_s^2 in the interval $(0, 1)$ for expansion of the universe. From figure 17, we have observed that v_s^2 decreases smoothly but lies within 0.2 and 0.82. So we can conclude that MCJG and MCAG are both classically stable.

References

- [1] S. J. Perlmutter et al., *Nature* 391, 51 (1998).
- [2] S. Perlmutter, [Supernova Cosmology Project Collaboration], *Astrophys. J.* 517, 565 (1999).
- [3] A. G. Riess et al. [Supernova Search Team Collaboration], *Astron. J.* 116, 1009 (1998).
- [4] D. J. Eisenstein and W. Hu, *Astrophys. J.* 496, 605 (1998).
- [5] D. J. Eisenstein, et al, *Astrophys. J.* 633, 560 (2005).
- [6] S. Bridle et al, *Science* 299, 1532 (2003).
- [7] D. N. Spergel et al (WMAP Collaboration), *Astrophys. J. Suppl. Ser.* 148, 175 (2003).
- [8] E. Komatsu et al. [WMAP Collaboration], *Astrophys. J. Suppl.* 180, 330 (2009).
- [9] P. A. R. Ade et al [Planck Collaboration], *Astron. Astrophys.* 594, A14 (2016).
- [10] P. J. E. Peebles and B. Ratra, *Rev. Mod. Phys.* 75, 559 (2003) 559.
- [11] T. Padmanabhan, *Phys. Rep.* 380, 2003 (2003).
- [12] E. J. Copeland, M. Sami and S. Tsujikawa, *Int. J. Mod. Phys. D* 15, 1753 (2006).
- [13] R. R. Caldwell and M. Kamionkowski, *Ann. Rev. Nucl. Part. Sci.* 59, 397 (2009).
- [14] S. Weinberg, *Rev. Mod. Phys.* 61, 1 (1989).
- [15] C. Armendariz-Picon, V. Mukhanov and P. J. Steinhardt, *Phys. Rev. D* 63, 103510 (2001).
- [16] R. R. Caldwell, *Phys. Lett. B* 545, 23 (2002).
- [17] E. Elizalde, S. Nojiri, and S. D. Odintsov, *Phys. Rev. D* 70, 043539 (2004).
- [18] R. R. Caldwell, R. Dave and P. J. Steinhardt, *Phys. Rev. Lett.* 80, 1582 (1998).
- [19] P. J. E. Peebles and B. Ratra, *Astrophys. J.* 325, L17 (1988).
- [20] S. Tsujikawa, *Class. Quantum Grav.* 30, 214003 (2013).
- [21] K. Bamba, S. Capozziello, S. Nojiri, and S. D. Odintsov, *Astrophys. Space Sci.* 342, 155 (2012).
- [22] Y. Chen, C.-Q. Geng, S. Cao, Y.-M. Huang, and Z.-H. Zhu, *JCAP* 2015, 010 (2015).
- [23] V. Smer-Barreto and A. R. Liddle, *JCAP* 2017, 023 (2017).
- [24] B. Ratra and P. J. E. Peebles, *Phys. Rev. D* 37, 3406 (1988).
- [25] C. Wetterich, *Nucl. Phys. B* 302, 668 (1988).

- [26] C. Armendariz-Picon, V. F. Mukhanov and P. J. Steinhardt, Phys. Rev. Lett. 85, 4438 (2000).
- [27] A. Sen, JHEP 0207, 065 (2002).
- [28] B. Feng, X. L. Wang and X. M. Zhang, Phys. Lett. B 607, 35 (2005).
- [29] Z. K. Guo, Y. S. Piao, X. M. Zhang and Y. Z. Zhang, Phys. Lett. B 608, 177 (2005).
- [30] M. Gasperini et al, Phys. Rev. D 65, 023508 (2002).
- [31] B. Gumjudpai and J. Ward, Phys. Rev. D 80 023528 (2009).
- [32] J. Martin and M. Yamaguchi, Phys. Rev. D 77 123508 (2008).
- [33] H. Wei, R.G. Cai and D.F. Zeng, Class. Quantum Grav. 22 3189 (2005).
- [34] G. R. Dvali, G. Gabadadze and M. Porrati, Phys. Lett. B 484, 112 (2000).
- [35] T. Jacobson and D. Mattingly, Phys. Rev. D 64, 024028 (2001).
- [36] M. C. B. Abdalla, S. Nojiri and S. D. Odintsov, Class. Quantum Grav. 22, L35 (2005).
- [37] S. Nojiri and S. D. Odintsov, Phys. Lett. B631, 1 (2005).
- [38] P. Horava, JHEP 0903, 020 (2009).
- [39] J. D. Barrow, Phys. Rev. D 85, 047503 (2012).
- [40] X. Meng and X. Du, Phys. Lett. B 710, 493 (2012).
- [41] S. Tsujikawa, Lect. Notes Phys. 800 99 (2010).
- [42] A. Kamenshchik, U. Moschella, and V. Pasquier, Phys. Lett. B 511, 265 (2001).
- [43] N. Bilic, G. B. Tupper and R. D. Viollier, Phys. Lett. B 535, 17 (2002).
- [44] V. Gorini, A. Kamenshchik, U. Moschella and V. Pasquier, gr-qc/0403062.
- [45] M. C. Bento, O. Bertolami and A. A. Sen, Phys. Rev. D 66, 043507 (2002).
- [46] M. Makler, S. Q. de Oliveira and I. Waga, Phys. Lett. B 555, 1 (2003).
- [47] V. Gorini, A. Kamenshchik and U. Moschella, Phys. Rev. D 67, 063509 (2003).
- [48] H. B. Benaoum, hep-th/0205140.
- [49] U. Debnath, A. Banerjee and S. Chakraborty, Class. Quantum Grav. 21 5609 (2004).
- [50] Z. K. Guo and Y. Z. Zhang, Phys. Lett. B 645, 326 (2007).
- [51] U. Debnath, Astrophys. Space Sci. 312, 295 (2007).
- [52] X. -H. Zhai, Y. -D. Xu and X. -Z. Li, Int. J. Mod. Phys. D 15, 1151 (2006).
- [53] M. C. Bento, O. Bertolami and A. A. Sen, Phys. Rev. D 67, 063003 (2003).

- [54] M. C. Bento, O. Bertolami and A. A. Sen, *Phys. Lett. B* 575, 172 (2003).
- [55] L. Amendola, F. Finelli, C. Burigana and D. Carturan, *JCAP* 0307, 005 (2003).
- [56] D. -J. Liu and X. -Z. Li, *Chin. Phys. Lett.* 22, 1600 (2005).
- [57] J. Lu, L. Xu, J. Li, B. Chang, Y. Gui and H. Liu, *Phys. Lett. B* 662, 87 (2008).
- [58] S. Chakraborty, U. Debnath and C. Ranjit, *Eur. Phys. J. C* 72, 2101 (2012).
- [59] B. C. Paul, P. Thakur and M. M. Verma, *Pramana* 81, 691 (2013).
- [60] U. Debnath, *Adv. High Energy Phys.* 2014, 653630 (2014).
- [61] C. Ranjit, P. Rudra and U. Debnath, *Can. J. Phys.* 92, 1667 (2014).
- [62] U. Debnath, *Int. J. Theor. Phys.* 54, 22 (2015).
- [63] U. Debnath, *Phys. Dark Univ.* 31, 100764 (2021).
- [64] J. R. Villanueva, *JCAP* 07, 045 (2015).
- [65] J. R. Villanueva and E. Gallo, *Eur. Phys. J. C* 75, 256 (2015).
- [66] A. G. Cadavid and J. R. Villanueva, *JCAP* 12, 044 (2020).
- [67] H. Yu, B. Ratra and F. Y. Wang, *Astrophys. J.* 856, 3 (2018).
- [68] M. Moresco, R. Jimenez, L. Verde, L. Pozzetti, A. Cimatti and A. Citro, *Astrophys. J.* 868, 84 (2018).
- [69] J. Magana, M. H. Amante, M. A. Garcia-Aspeitia and V. Motta, *MNRAS* 476, 1036 (2018).
- [70] G. S. Sharov, V. O. Vasiliev, *Mathematical Modelling and Geometry* 6, 1 (2018).
- [71] Y. -Y. Xu and X. Zhang, *Eur. Phys. J. C* 76, 588 (2016).
- [72] Y. Wang and M. Dai, *Phys. Rev. D* 94, 083521 (2016).
- [73] W. Hu and N. Sugiyama, *Astrophys. J.* 471, 542 (1996).
- [74] F. Beutler et al, *Mon. Not. Roy. Astron. Soc.* 416, 3017 (2011).
- [75] A. J. Ross et al, *Mon. Not. Roy. Astron. Soc.* 449, 835 (2015).
- [76] L. Anderson et al [BOSS Collaboration], *Mon. Not. Roy. Astron. Soc.* 441, 24 (2014).
- [77] M. Kowalaski et al, *Astrophys. J.* 686, 749 (2008).
- [78] D. M. Scolnic et al., *Astrophys. J.* 859, 101 (2018).
- [79] M. Betoule et al [SDSS Collaboration], *Astron. Astrophys.* 568, A22 (2014).
- [80] R. Amanullah, *Astrophys. J.* 716, 712 (2010).
- [81] A. Al Mamon and S. Das, *Eur. Phys. J. C* 76, 135 (2016).

- [82] R. G. Cai, Z. L. Tuo, H. B. Zhang and Q. Su, *Phys. Rev. D* 84, 123501 (2011).
- [83] U. Debnath and K. Bamba, *Eur. Phys. J. C* 79, 722 (2019).
- [84] H. Akaike, *IEEE Trans. Autom. Control* 19, 716 (1974).
- [85] G. Schwarz, *Ann. Stat.* 6, 461 (1978).
- [86] D. J. Spiegelhalter, N. G. Best, B. P. Carlin, A. Van Der Linde, *J. R. Stat. Soc.* 64, 583 (2002).
- [87] A. R. Liddle, *Mon. Not. Roy. Astron. Soc.* 377, L74 (2007).
- [88] K. Anderson, *Model selection and multimodel inference: a practical information-theoretic approach*, 2nd edn. Springer, New York (2002).
- [89] K. P. Burnham and D. R. Anderson, *Sociological Methods and Research* 33, 261 (2004).
- [90] N. Sugiura, *Commun. Stat. A Theor.* A7, 13 (1978).
- [91] S. Pan, A. Mukherjee and N. Banerjee, *Mon. Not. R. Astron. Soc.* 477, 1189 (2018).
- [92] C. Escamilla-Rivera and S. Capozziello, *Int. J. Mod. Phys. D* 28, 1950154 (2019).
- [93] S. Mandal, D. Wang and P. K. Sahoo, *Phys. Rev. D* 102, 124029 (2020).
- [94] S. K. J. Pacif, S. Arora and P. K. Sahoo, *Phys. Dark Universe* 32, 100804 (2021).
- [95] V. Sahni, T. D. Saini, A. A. Starobinsky and U. Alam, *JETP Lett.* 77, 201 (2003).
- [96] U. Alam, V. Sahni, T. D. Saini, A. A. Starobinsky, *Mon. Not. R. Astron. Soc.* 344, 1057 (2003).
- [97] V. Sahni et al., *Phys. Rev. D* 78 103502 (2008).